Exploiting Spectral Regrowth for Channel Identification

Kuang Cai, Hongbin Li, and Joseph Mitola, III

***Abstract*—In modern communication systems, power amplifiers (PAs) are important components and inherently nonlinear. The nonlinearity of the PA causes bandwidth expansion of the communication signal, often referred to as *spectral regrowth*, at the PA output. Conventionally, spectral regrowth is treated as a distortion, and a range of compensation and filtering techniques have been considered to mitigate its effect. In this paper, we propose to exploit spectral regrowth to enhance channel identification accuracy. Our approach is motivated by the fact that the nonlinearly amplified communication signal carries more bandwidth and allows better probing of the channel. We introduce an iterative algorithm which jointly estimates the PA characteristics and the channel impulse response. The effectiveness of the proposed algorithm is illustrated by computer simulation.**

***Index Terms*—Channel identification, nonlinear power amplifier, spectral regrowth.**

I. Introduction

POWER AMPLIFIERS (PAs) are important components in communication systems. PAs are also major sources of nonlinearity in such systems. A PA produces bandwidth expansion of the communication signal. This phenomenon, called *spectral regrowth* or *spectral regeneration* [1]–[4], is caused by the creation of mixing products between the individual frequency components of the communication signal. Spectral regrowth is conventionally treated as a distortion since it may contribute to adjacent channel interference [5], [6]. This has led to numerous studies on how to mitigate the effect of spectral regrowth via predistortion and filtering techniques [7]–[13].

However, spectral regrowth can be beneficial from the perspective of channel characterization and identification. It is known how well the channel can be estimated is fundamentally related to the bandwidth of the probing signal. This is the basic idea behind radar which often employs a wideband chirp signal to sound the environment. While a narrowband communication signal is by design not an ideal channel probing signal, the extra bandwidth induced by nonlinear power amplification holds the potential of improving channel estimation.

Manuscript received March 12, 2014; revised April 28, 2014; accepted May 08, 2014. Date of publication May 14, 2014; date of current version May 20, 2014. The associate editor coordinating the review of this manuscript and approving it for publication was Prof. Zoltan Safar.

K. Cai and H. Li are with the Department of Electrical and Computer Engineering, Stevens Institute of Technology, Hoboken, NJ 07030 USA (e-mail: kcai@stevens.edu; Hongbin.Li@stevens.edu).

J. Mitola III is with Mitola's STATISfaction, St. Augustine, FL 32080 USA (e-mail: jmitola@ieee.org).

Color versions of one or more of the figures in this paper are available online at http://ieeexplore.ieee.org.

Digital Object Identifier 10.1109/LSP.2014.2323943

In this letter, we investigate how to exploit spectral regrowth for channel identification in communications. An important question that needs to be addressed is how much of the spectral regrowth content can be utilized to benefit channel identification. The question arises from the fact that for a PA with moderate nonlinearity, the power spectral density (PSD) of the PA output decreases with increasing frequency in outband. To answer this question, we consider a receiver front end (baseband equivalent) equipped with a lowpass filter (LPF) which has a variable cutoff frequency. By increasing the cutoff frequency, more of the spectral regrowth content of the signal is utilized for channel identification and, meanwhile, there is more noise entering the system. It is therefore necessary to examine the trade-off and determine the best cutoff frequency from both estimation accuracy and complexity points of view.

Both the PA characteristics and the multipath channel are assumed unknown in this work. We develop a joint estimator which iteratively estimates the PA characteristics and the multipath channel coefficients. To benchmark the performance of the proposed estimator, we also derive the Cramér-Rao bound (CRB) for the estimation problem, which gives the best achievable performance of any unbiased estimator.

The rest of the paper is organized as follows. In Section II, we introduce the system model and formulate the problem of interest. In Section III, we present our proposed method. The related numerical results are presented in Section IV. Finally, the paper is concluded in Section V.

Notation: Vectors (matrices) are denoted by boldface lower (upper) case letters; $*$ denotes the convolution; $\otimes$ denotes the Kronecker product; superscripts $(\cdot)^T$ and $(\cdot)^H$ denote the transpose and conjugate transpose respectively; $\mathbf{I}_N$ denotes an $N \times N$ identity matrix; $\hat{A}$ denotes an estimate of A.

II. Problem Statement

Consider a basedband linearly modulated signal $s(t)$ consisting of L symbols b_n given by

$$s(t) = \sum_{n=0}^{L-1} b_n p(t - nT) \tag{1}$$

where b_n is the nth symbol, $p(t)$ the pulse shaping filter and T the symbol period. The signal is power amplified and sent across a multipath channel with impulse response $h(t)$. Assume that the channel $h(t)$ spans M symbol periods:

$$h(t) = \sum_{m=0}^{M} h_m \delta(t - t_m) \tag{2}$$

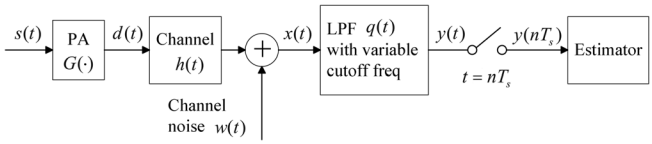

Fig. 1. Baseband system model.

where $t_m = mT$. Then, the received signal is

$$x(t) = \sum_{m=0}^{M} h_m G[s(t - mT)] + w(t) \tag{3}$$

where $G(\cdot)$ denotes the nonlinear PA input/output relation and $w(t)$ the additive Gaussian white channel noise. Let $d(t) = G[s(t)]$. Consider the polynomial model which is commonly used to characterize memoryless PAs in baseband [4], [5], [14], [15]:

$$d(t) = \sum_{j=0}^{J} \alpha_{2j+1} s(t)|s(t)|^{2j} \tag{4}$$

where α_{2j+1} denotes the jth polynomial coefficient which is unknown and needs to be estimated. The memoryless model is employed for many PAs used in practice, such as the traveling wave tube (TWT) amplifier, solid state power amplifier (SSPA) and soft-envelope limiter (SEL) [16]. Referring to (4), the higher order ($j > 0$) components bring in spectral regrowth. Suppose that the message signal $s(t)$ has a bandwidth W_s. It is easy to see that the PA output $d(t)$ has an expanded bandwidth $W_d = (2J + 1)W_s$.

The problem of interest is to jointly estimate the multipath channel response h_m and PA characteristics α_{2j+1} from the received signal $x(t)$ given knowledge of the L training symbols b_n and pulse shaping filter $g(t)$.

III. Proposed Method

A. Receiver Structure and Discrete-Time Model

The nonlinearly amplified signal $d(t)$ has more bandwidth than the original signal $s(t)$ and can potentially lead to better channel identification performance. To quantify the effect of bandwidth on channel identification, we apply an LPF with variable cutoff frequency B (in Hz) as the receiver front end filter. We examine the estimation performance as a function of B. The LPF output can be written as

$$\begin{aligned} y(t) &= q(t) * x(t) \\ &= q(t) * d(t) * h(t) + q(t) * w(t) \end{aligned} \tag{5}$$

where $q(t)$ is the impulse response of the LPF. Fig. 1 shows the diagram of the system model in baseband.

The system output is sampled at the Nyquist rate $2B$ relative to the LPF bandwidth. Let $T_s = 1/2B$ denote the sampling interval, $P = T/T_s \geq 1$ the oversampling rate, and $v(t)$ the filtered noise. From (3) and (5), the output sample is given by

$$\begin{aligned} y(nT_s) = \sum_{m=0}^{M} h_m \int_{\tau=-\infty}^{\infty} d(\tau - mT) q(nT_s - \tau) d\tau \\ + v(nT_s). \end{aligned} \tag{6}$$

Suppose the estimation is based on an observation of $y(t)$ for $N = L - M$ symbol intervals, where the initial M symbol intervals and tailing M symbol intervals are not used for estimation. To obtain a discrete-time model, we approximate the integral in (6) by summation with a small step size Δ. Let $K = T_s/\Delta$. Note that Δ is chosen as a small fraction of T_s such that K as well as PK, NPK and MPK, which are dimensions of several vectors/matrices defined below, are integers. Then, (6) can be expressed by

$$\begin{aligned} y(nT_s) \approx \sum_{m=0}^{M} h_m \sum_{i=0}^{NPK-1} \Delta d(i\Delta - mT) q(nT_s - i\Delta) \\ + v(nT_s). \end{aligned} \tag{7}$$

Let $d_i \triangleq d(i\Delta), q_i \triangleq q(i\Delta), y_n \triangleq y(nT_s)$ and $v_n \triangleq v(nT_s)$. The output samples, filtered noise samples and the channel response in vector form are given by:

$$\begin{aligned} \mathbf{y} &\triangleq [\, y_0 \quad y_1 \quad \cdots \quad y_{NP-1} \,]^T \\ \mathbf{v} &\triangleq [\, v_0 \quad v_1 \quad \cdots \quad v_{NP-1} \,]^T \\ \mathbf{h} &\triangleq [\, h_0 \quad h_1 \quad \cdots \quad h_M \,]^T. \end{aligned} \tag{8}$$

Then, we have the system output in matrix/vector form as

$$\mathbf{y} = \mathbf{QDh} + \mathbf{v} \tag{9}$$

where $\mathbf{Q}$ is an $NP \times NPK$ matrix

$$\mathbf{Q} = \begin{bmatrix} q_0 & q_{-1} & \cdots & q_{-NPK+1} \\ q_K & q_{K-1} & \cdots & q_{(1-NP)K+1} \\ \vdots & \vdots & \ddots & \vdots \\ q_{(NP-1)K} & q_{(NP-1)K-1} & \cdots & q_{-K+1} \end{bmatrix}$$

and $\mathbf{D}$ is an $NPK \times (M + 1)$ matrix given by

$$\mathbf{D} = \begin{bmatrix} d_0 & d_{-PK} & \cdots & d_{-MPK} \\ d_1 & d_{-PK+1} & \cdots & d_{-MPK+1} \\ \vdots & \vdots & \ddots & \vdots \\ d_{NPK-1} & d_{(N-1)PK-1} & \cdots & d_{(N-M)PK-1} \end{bmatrix}.$$

B. Joint Channel and PA Estimation

Equation (9) shows how the receiver output $\mathbf{y}$ depends on the channel response $\mathbf{h}$. Next, we explicitly show the dependence of $\mathbf{y}$ on the PA characteristics $\{\alpha_{2j+1}\}$. In particular, by defining: $s_i \triangleq s(i\Delta)$,

$$\begin{aligned} \mathbf{s}_i &\triangleq [s_i \; s_i|s_i|^2 \cdots s_i|s_i|^{2J}]^T \\ \boldsymbol{\alpha} &\triangleq [\alpha_1 \; \alpha_3 \cdots \alpha_{2J+1}]^T \end{aligned} \tag{10}$$

we can write $\mathbf{D}$ as

$$\mathbf{D} = \mathbf{S}\mathcal{A} \tag{11}$$

where $\mathcal{A} = \mathbf{I}_{M+1} \otimes \boldsymbol{\alpha}$, and $\mathbf{S}$ is an $NPK \times (M + 1)$ matrix

$$\mathbf{S} = \begin{bmatrix} \mathbf{s}_0^T & \mathbf{s}_{-PK}^T & \cdots & \mathbf{s}_{-MPK}^T \\ \mathbf{s}_1^T & \mathbf{s}_{-PK+1}^T & \cdots & \mathbf{s}_{-MPK+1}^T \\ \vdots & \vdots & \ddots & \vdots \\ \mathbf{s}_{NPK-1}^T & \mathbf{s}_{(N-1)PK-1}^T & \cdots & \mathbf{s}_{(N-M)PK-1}^T \end{bmatrix}.$$

Referring to (11), our system model (9) becomes

$$\mathbf{y} = \mathbf{QS}\mathcal{A}\mathbf{h} + \mathbf{v}. \tag{12}$$

A simple approach is to estimate $\mathcal{A}\mathbf{h}$ as an unknown vector without considering its structure. Specifically, since the noise samples $v(nT_s)$ are obtained at the Nyquist sampling rate $2B$ and therefore are independent and identically distributed Gaussian, the unstructured maximum likelihood estimate (MLE) reduces to the least squares estimate (LSE):

$$\widehat{\mathcal{A}\mathbf{h}} = [(\mathbf{QS})^H(\mathbf{QS})]^{-1}(\mathbf{QS})^H\mathbf{y}. \tag{13}$$

Let $\widehat{\mathcal{A}\mathbf{h}}$ be decomposed as

$$\widehat{\mathcal{A}\mathbf{h}} = [(\widehat{h_0\boldsymbol{\alpha}})^T\ (\widehat{h_1\boldsymbol{\alpha}})^T \cdots (\widehat{h_M\boldsymbol{\alpha}})^T]^T. \tag{14}$$

We can construct the following rank-1 matrix

$$\widehat{\boldsymbol{\alpha}\mathbf{h}^T} = [\widehat{h_0\boldsymbol{\alpha}}\ \widehat{h_1\boldsymbol{\alpha}} \cdots \widehat{h_M\boldsymbol{\alpha}}]. \tag{15}$$

Note that there is an inherent multiplicative ambiguity in separating $\mathbf{h}$ and $\boldsymbol{\alpha}$. To resolve the ambiguity, we assume some knowledge of the PA is available, e.g., the linear gain α_1 of the PA, which is often known in practice. Such knowledge can be obtained through a calibration process [17]. Then, we can separate the estimates of $\mathbf{h}$ and $\boldsymbol{\alpha}$ from the singular value decomposition (SVD) of (15) (more details later).

The above non-structured estimator was found to be unsatisfactory, in particular when the signal-to-noise ratio (SNR) is low. Next, we present an enhanced estimator by iteratively estimating $\mathbf{h}$ and $\boldsymbol{\alpha}$ in succession, using the non-structured estimates to initialize the iteration. Specifically, note that

$$\mathcal{A}\mathbf{h} = \mathbf{H}\boldsymbol{\alpha} \tag{16}$$

where $\mathbf{H} = \mathbf{h} \otimes \mathbf{I}_{J+1}$. Then, we can write (12) as

$$\mathbf{y} = \mathbf{QS}\mathcal{A}\mathbf{h} + \mathbf{v} = \mathbf{QSH}\boldsymbol{\alpha} + \mathbf{v}. \tag{17}$$

Equation (17) shows that given either $\boldsymbol{\alpha}$ or $\mathbf{h}$, the other can be estimated by the LSE. Hence, our iterative estimation algorithm consists of the following steps:

Step 1 (Initialization). Set $k = 0$. Compute the SVD of (15)

$$\widehat{\boldsymbol{\alpha}\mathbf{h}^T} = \mathbf{U}\boldsymbol{\Sigma}\mathbf{V}^T. \tag{18}$$

Denote the first column of $\mathbf{U}$ and its first element as $\mathbf{u}$ and u_1, respectively. Using the fact that α_1 is known (say, $\alpha_1 = a$), we have $\hat{\boldsymbol{\alpha}}^{(0)} = \frac{a}{u_1}\mathbf{u}$;

Step 2. Set $k = k + 1$. Referring to (17), apply LSE to compute the estimates of $\mathbf{h}$ and $\boldsymbol{\alpha}$ as follows:

$$\begin{aligned}
\hat{\mathbf{h}}^{(k)} &= [(\mathbf{QS}\hat{\mathcal{A}}^{(k-1)})^H(\mathbf{QS}\hat{\mathcal{A}}^{(k-1)})]^{-1}(\mathbf{QS}\hat{\mathcal{A}}^{(k-1)})^H\mathbf{y} \\
\tilde{\boldsymbol{\alpha}}^{(k)} &= [(\mathbf{QS}\hat{\mathbf{H}}^{(k)})^H(\mathbf{QS}\hat{\mathbf{H}}^{(k)})]^{-1}(\mathbf{QS}\hat{\mathbf{H}}^{(k)})^H\mathbf{y} \\
\hat{\boldsymbol{\alpha}}^{(k)} &= \frac{a}{\tilde{\alpha}_1^{(k)}}\tilde{\boldsymbol{\alpha}}^{(k)}
\end{aligned} \tag{19}$$

where $\hat{\mathcal{A}}^{(k-1)}$ and $\hat{\mathbf{H}}^{(k)}$ are constructed from $\hat{\boldsymbol{\alpha}}^{(k-1)}$ and $\hat{\mathbf{h}}^{(k)}$, respectively, and the last normalizing step is to impose the prior knowledge of $\alpha_1 = a$;

Step 3. Repeat Step 2 until the estimates of $\mathbf{h}$ and $\boldsymbol{\alpha}$ converge. In our simulation, we noticed the algorithm usually converges in $k \leq 5$ iterations.

C. CRB

To benchmark the proposed estimator, we calculate the corresponding Cramér-Rao bound which provides a lower bound on all unbiased estimators. Collect all unknown parameters in one vector:

$$\boldsymbol{\theta} = \begin{bmatrix} \mathbf{h} \\ \boldsymbol{\alpha} \end{bmatrix}. \tag{20}$$

Note that the LPF filter output noise $\mathbf{v}$ is spectrally white with covariance matrix

$$\boldsymbol{\Sigma}_{\mathbf{v}} = (N_0/2)(2B)\mathbf{I}_{NP} = N_0B\mathbf{I}_{NP} \tag{21}$$

where $N_0/2$ is the double-sided PSD of $w(t)$. Referring to (17), the Fisher information matrix (FIM) is given by [18]

$$\mathbf{J} = \frac{1}{N_0B}[\mathbf{QS}\mathcal{A}\ \mathbf{QSH}]^T[\mathbf{QS}\mathcal{A}\ \mathbf{QSH}]. \tag{22}$$

Due to the aforementioned multiplicative ambiguity between $\mathbf{h}$ and $\boldsymbol{\alpha}$, $\mathbf{J}$ is singular and cannot be inverted to yield the CRB. A useful constrained CRB can be obtained by imposing the prior knowledge of α_1, which is also employed in our estimator. The constrained CRB is computed by using the approach discussed in [19]. Specifically, construct a constraint function:

$$c(\boldsymbol{\theta}) = \alpha_1 - a \tag{23}$$

where $c(\boldsymbol{\theta}) = 0$. Let

$$\mathbf{c}(\boldsymbol{\theta}) = \partial c(\boldsymbol{\theta})/\partial\boldsymbol{\theta}^T. \tag{24}$$

Find out a matrix whose columns form a basis for the nullspace of $\mathbf{c}(\boldsymbol{\theta})$, and denote it as $\mathbf{W}$. The constrained CRB is given by

$$\mathcal{CRB}[\boldsymbol{\theta}; c(\boldsymbol{\theta}) = 0] = \mathbf{W}(\mathbf{W}^T\mathbf{J}\mathbf{W})^{-1}\mathbf{W}^T. \tag{25}$$

IV. Numerical Results

In our simulation, we use binary phase shift keying (BPSK) using root-raised-cosine (RRC) pulse $p(t)$ with roll-off factor $\beta = 0.5$. The nonlinear PA is a 5-th order amplifier with coefficients taken from [20, Table 1]. The impulse response of the multipath channel is given by: $h(t) = \delta(t) - 0.7\delta(t - T) + 0.4\delta(t - 2T) - 0.2\delta(t - 3T)$. The SNR is defined as: $\text{SNR} = \frac{E_b}{N_0/2}$, where E_b denotes the signal energy per symbol.

We compare the estimation performance at five different cutoff frequencies, $B = W_s, 2W_s, 3W_s, 4W_s$ and $5W_s$, where $W_s = \frac{1+\beta}{2T}$ denotes the message signal bandwidth. Note that $B = W_s$ corresponds to the ***conventional approach*** which does not employ the spectral regrowth for identification, where the other cases use the spectral regrowth. For all cases, we use $L = 29$ training symbols for estimation. As performance metric, we use the normalized mean squared error (MSE) $E\{\|\hat{\mathbf{a}} - \mathbf{a}\|^2/\|\mathbf{a}\|^2\}$ obtained from 2000 independent trials, where $\mathbf{a}$ denotes either the channel $\mathbf{h}$ or PA coefficients $\boldsymbol{\alpha}$.

Fig. 2 shows the results for PA characteristics and channel estimation. It is observed that for both PA and channel estimation, the proposed estimator asymptotically (for high SNR) achieves the CRB and is therefore statistically efficient. The estimation

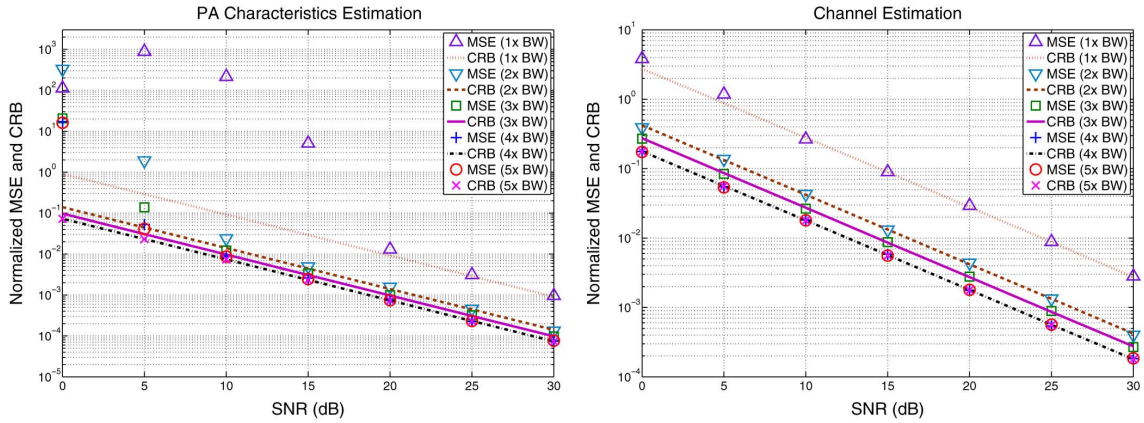

(a) (b)

Fig. 2. MSE and CRB for the estimation of (a) PA coefficients; and (b) channel response.

accuracy is improved when the spectral regrowth is utilized. However, the benefit of spectral regrowth is seen to diminish as the cutoff frequency B of the LPF increases. In particular, almost identical estimation accuracy in terms of both the MSE and CRB is obtained at $B = 4W_s$ and $B = 5W_s$. As noted before, as the cutoff and sampling frequency increases, on one hand we have more signal samples and include more of the useful signal energy for estimation, while on the other hand each sample is noisier as the noise variance increases with B (see (21)). The diminishing gain is precisely due to the trade-off effect between the signal and noise as the bandwidth of the filter changes. For the considered case, it appears $B = 3W_s$ or $4W_s$ is the best choice for estimation for the considered setup since a larger B brings little performance improvement but incurs a higher complexity. Finally, it is noted that the proposed algorithm converges typically in less than 5 iterations for all cases considered, and the convergence rate is slightly faster (in 2 to 3 iterations) for larger B and/or higher SNR.

V. Conclusion

In communication systems with nonlinear PA components, spectral regrowth is conventionally treated as a distortion. Since useful signal energy is contained in the expanded bandwidth due to spectral regrowth, utilizing spectral regrowth holds the benefit of improving the channel estimation accuracy. In this work, we proposed an iterative channel identification algorithm by exploiting spectral regrowth. Our results show that compared with the conventional approach which cuts out the outband energy of the received signal, significant improvement can be obtained by using three to four times the message signal bandwidth for channel identification. However, it is noted that increasing the bandwidth beyond this range seems not recommended due to the diminishing gain and additional complexity incurred to the estimation algorithm.

References

[1] S. A. Maas, "Volterra analysis of spectral regrowth," *IEEE Microwave Guided Wave Lett.*, vol. 7, no. 7, pp. 192–193, Jul. 1997.

[2] V. Aparin, "Analysis of CDMA signal spectral regrowth and waveform quality," *IEEE Trans. Microwave Theory Techn.*, vol. 49, no. 12, pp. 2306–2314, Dec. 2001.

[3] W. V. Moer, Y. Rolain, and A. Geens, "Measurement-based nonlinear modeling of spectral regrowth," *IEEE Trans. Instrum. Meas.*, vol. 50, no. 6, pp. 1711–1716, Dec. 2001.

[4] E. Cottais, Y. Wang, and S. Toutain, "Spectral regrowth analysis at the output of a memoryless power amplifier with multicarrier signals," *IEEE Trans. Commun.*, vol. 56, no. 7, pp. 1111–1118, Jul. 2008.

[5] G. T. Zhou and J. S. Kenney, "Predicting spectral regrowth of nonlinear power amplifiers," *IEEE Trans. Commun.*, vol. 50, no. 5, pp. 718–722, May 2002.

[6] C. Nader, P. Händel, and N. Björsell, "Peak-to-average power reduction of OFDM signals by convex optimization: Experimental validation and performance optimization," *IEEE Trans. Instrum. Meas.*, vol. 60, no. 2, pp. 473–479, Feb. 2011.

[7] L. Anttila, P. Händel, and M. Valkama, "Joint mitigation of power amplifier and I/Q modulator impairments in broadband direct-conversion transmitters," *IEEE Trans. Microwave Theory Techn.*, vol. 58, no. 4, pp. 730–739, Apr. 2010.

[8] J. Zeleny, C. Dehos, P. Rosson, and A. Kaiser, "Receiver-aided predistortion of power amplifier non-linearities in cellular networks," *IET Sci. Meas. Technol.*, vol. 6, no. 3, pp. 168–175, 2012.

[9] S. H. Ahn, S. Choi, E. R. Jeong, and Y. H. Lee, "Compensation for power amplifier nonlinearity in the presence of local oscillator coupling effects," *IEEE Commun. Lett.*, vol. 16, no. 5, pp. 600–603, May 2012.

[10] M. Cabarkapa, N. Neskovic, A. Neskovic, and D. Budimir, "Adaptive nonlinearity compensation technique for 4G wireless transmitters," *Electron. Lett.*, vol. 48, no. 20, pp. 1308–1309, Sep. 2012.

[11] R. N. Braithwaite, "A combined approach to digital predistortion and crest factor reduction for the linearization of an RF power amplifier," *IEEE Trans. Microwave Theory Techn.*, vol. 61, no. 1, pp. 291–302, Jan. 2013.

[12] O. A. Gouba and Y. Louët, "Adding signal for peak-to-average power reduction and predistortion in an orthogonal frequency division multiplexing context," *IET Signal Process.*, vol. 7, no. 9, pp. 879–887, 2013.

[13] X. Yu and H. Jiang, "Digital predistortion using adaptive basis functions," *IEEE Trans. Circuits Syst. I: Regular Papers*, vol. 60, no. 12, pp. 3317–3327, Dec. 2013.

[14] S. Benedetto and E. Biglieri, *Principles of Digital Transmission with Wireless Applications*. New York, NY, USA: Kluwer Academic/Plenum, 1999.

[15] R. Raich and G. T. Zhou, "Orthogonal polynomials for complex gaussian processes," *IEEE Trans. Signal Process.*, vol. 52, no. 10, pp. 2788–2797, Oct. 2004.

[16] J. Qi and S. Aïssa, "Analysis and compensation of power amplifier nonlinearity in MIMO transmit diversity systems," *IEEE Trans. Veh. Technol.*, vol. 59, no. 6, pp. 2921–2931, Jul. 2010.

[17] G. Lazzarin, S. Pupolin, and A. Sarti, "Nonlinearity compensation in digital radio systems," *IEEE Trans. Commun.*, vol. 42, no. 2/3/4, pp. 988–999, Feb./Mar./Apr. 1994.

[18] S. M. Kay, *Fundamentals of Statistical Signal Processing: Estimation Theory*. Upper Saddle River, NJ, USA: Prentice-Hall, 1993.

[19] P. Stoica and B. C. Ng, "On the Cramér-Rao bound under parametric constraints," *IEEE Signal Process. Lett.*, vol. 5, no. 7, pp. 177–179, Jul. 1998.

[20] G. T. Zhou and R. Raich, "Spectral analysis of polynomial nonlinearity with applications to RF power amplifiers," *EURASIP J. Appl. Signal Process.*, vol. 12, pp. 1831–1840, 2004.